SAND2011-2782C

Radar Cross Section Statistics of Ground Vehicles at Ku-band

Ann Marie Raynal*, Douglas L. Bickel, Michael M. Denton, Wallace J. Bow, Armin W. Doerry
Sandia National Laboratories, PO Box 5800, Albuquerque, NM, USA 87185-0519

ABSTRACT

Knowing the statistical characteristics of a target's radar cross-section (RCS) is crucial to the success of radar target detection algorithms. Open literature studies regarding the statistical nature of the RCS of ground vehicles focus primarily on simulations, scale model chamber measurements, or limited experimental data analysis of specific vehicles at certain frequencies. This paper seeks to expand the existing body of work on ground vehicle RCS statistics at Ku-band for ground moving target indication (GMTI) applications. We examine the RCS probability distributions of civilian and military vehicles, across aspect and elevation angle, for HH and VV polarizations, and at diverse resolutions, using experimental data collected at Ku-band. We further fit Swerling target models to the distributions and suggest appropriate detection thresholds for ground vehicles in this band.

Keywords: RCS, radar cross section, RCS distribution, RCS statistics, GMTI, vehicle RCS, vehicle radar cross section

1. INTRODUCTION

The detection of ground vehicles has been important for many decades for facility and battlefield monitoring of military vehicles, in particular. Civilian vehicles have become increasingly important for GMTI applications in recent years for border and terrorist surveillance, as well as traffic monitoring and automotive collision avoidance. An examination of the published literature yields some information on ground vehicle RCS statistics in certain radiolocation bands, such as X-band and millimeter wave. However, little information exists in the literature regarding the RCS statistics of ground vehicles at Ku-band. We chose to perform direct measurements of ground vehicles to augment the body of knowledge and compare results with the more abundant simulation and chamber data available in the literature. These efforts are discussed in subsequent chapters. Lastly, it should be noted that Ku-band was judiciously chosen for our study in support of current GMTI detection radars -- many of which operate in this band at the present time.

This paper is organized into four main parts. A review of the current literature on RCS statistics at Ku-band is provided in Section 2. A description of available data sets or experiments conducted to find direct measurements of ground vehicle RCS as a function of vehicle type, pose relative to the radar, polarization, resolution and clutter are outlined in Section 3. Experimental results regarding RCS distributions, statistics, and Swerling target models are given in Section 4. Conclusions are discussed in Section 5.

2. REVIEW OF THE STATE-OF-THE-ART

The University of Massachusetts Lowell, in collaboration with the National Ground Intelligence Center, have contributed extensively to the RCS literature on military ground vehicles through chamber scale-model and full-scale measurements at X-band and millimeter wave frequencies such as Ka and W-band. The German Aerospace Center (DLR) has conducted various experiments at C, L, and X-band for civilian ground vehicles.

Palubinskas and Runge[1] measured the RCS of a VW Golf V passenger car at X-band with VV polarization near 42-degree grazing. At cardinal angles the RCS measurements were usually above 0 dBsm, with values as high as 19 dBsm for the vehicle sides, 13 dBsm for the front, and 16 dBsm for the back. At oblique angles, the measured RCS was considerably less, with a mean below 0 dBsm and values as low as −18 dBsm. Over all angles, the mean RCS was 0.5 dBsm with a standard deviation of 7.1 dB. Variations of more than 10 dBsm were observed with as little as 0.35 degree aspect change, indicating high sensitivity to aspect angle.

Nixon, et al.[2] measured 11 full-size T-72 tanks at Ka-band at 5 degree grazing angle. They report a median value of 11.3 dBsm for VV polarization with a 12.3 dB standard deviation and 12.7 dBsm mean RCS. Results vary slightly for

*amrayna@sandia.gov; phone 1 505 284-3053; fax 1 505 844-0858; www.sandia.gov

horizontal polarization, which is no more than 1 dB higher, and different vehicle configurations, which change by no more than 3 dB. Plots show no measurements less than 7 dBsm and RCS peaks at cardinal angles near 20 dBsm and 25 dBsm for the front or back and sides of the tanks, respectively. Giles, et al.[3] measured both models and full-size tanks of several types at Ka-band. The various models exhibited median values from 11 to 16 dBsm at VV. Mean values were on the order of 2 dB higher, indicating perhaps larger deviations towards greater RCS than deviations to smaller RCS. HH polarization values tracked the VV values closely within 0.5 dB and no clear advantage of one polarization over the other.

Goyette, et al.[4] measured scaled models of a T-72 tank to determine X-band RCS characteristics of full-size tanks. They show data that indicates a median value in the neighborhood of 11 dBsm, with no data below 6 dBsm. RCS peaks at the cardinal angles of the tanks show values near 30 dBsm and 20 dBsm for the vehicle sides and front or back, respectively. They state that HH results are similar to VV and therefore do not bother providing comparisons of results amongst the two polarizations.

From Palubinskas, Runge, and Reinartz,[5, 6] RCS L-band data on 4 civilian vehicles at 42 deg. grazing show that HH and VV polarizations are similar in response across aspect, with strong RCS flashes at cardinal angles of the front, back and sides of the vehicles. HH polarization seems to yield slightly stronger returns for the majority of the aspect angles by about 2 dB. The authors insinuate that the responses are similar at X-band. VV returns at the cardinal angles at X-band averaged 7 dBsm for 7 different passenger vehicles at each cardinal angle.[7] Furthermore, cross-polarization results show much weaker RCS returns in the realm of -15 to 0 dBsm.[5, 6]

A study for vehicle collision sensors by M. Haruta, H. Ishizaka, O. Hashimoto, J. Ueyama, and K. Wada[8] at millimeter waves, suggests 4 to 5 dB stronger HH returns over VV for a bus, but not a 4-ton truck at the -5 to 5-degree azimuth angles of the back of the vehicle and low grazing. The RCS ranges from 17-37 dBsm at VV versus 15-32 dBsm at HH for the truck and 15-39 dBsm at VV versus 12-51 dBsm at HH for the bus.

Lees and Davies[9] report on the RCS variation of a tank-like target at 14.11GHz as a function of azimuth angle at 7-degree grazing with horizontal polarization. The RCS fluctuates minimally by about 2 dB around a mean of -10 dBsm as a function of most angles. The exceptions to this behavior occur at the front, rear, and sides of the tank, where strong dihedral flash scattering mechanisms between the ground and vehicle produce sharp RCS peaks of 15 to 30 dBsm. At L-band with horizontal polarization, Papadopoulos, et al.[10] show similar behavior using the electromagnetic solver FEKO for a main battle tank model, though their mean RCS for most angles is near 10 dBsm.

Papadopoulos and Mulgrew[11] further report on the probability density function (PDF) and cumulative density function (CDF) of a main battle tank and armored personnel carrier model at L-band using FEKO. The PDFs in general range from -10 to 40 dBsm with the most probable values occurring from 0 to 10 dBsm. The CDF of the main battle tank confirms that the median RCS value is 10 dBsm, as observed in their angular RCS results. The authors conclude that the PDF of ground vehicles varies by vehicle type and collection geometry parameters, particularly pose. They also demonstrate that the PDF can be multimodal in some cases, rather than a Gaussian distribution.

Taken in total, the statistical data suggests that there is not a strong frequency-dependence in the RCS of tank-like vehicles. This observation was also made by Palubinskas, et al.[5] for civilian passenger vehicles across C, L, and X-band.

In summary, we expect the following RCS behavior based on the literature. The RCS variation with polarization should be minimal between HH and VV. Cross-polarization values should be lower than co-polarization values by an order of magnitude. RCS variation as a function of azimuth should be dominated by strong flashes at cardinal angles in the 15-30 dBsm range, with approximately constant RCS at oblique angles. The range of RCS values can fall between -18 dBsm and 40 dBsm with the median value near 10 dBsm and a standard deviation upwards of 7 dB. Civilian vehicle RCS is expected to be about an order of magnitude lower than that of large vehicles. Frequency dependence is minimal.

3. VEHICLE RCS DATA SETS AND EXPERIMENTS

The ground vehicle RCS data sets and experiments that we conducted are described next. In all cases, we used stationary vehicle RCS results, with the assumption that the RCS of moving vehicles for GMTI is similar.

3.1. Large Organizational Vehicles

We utilized the Sandia National Laboratories automatic target recognition database to acquire the RCS of multiple vehicles in various configurations -- across many aspect angles, look angles, polarizations, resolutions, and scene clutter.

Typical synthetic aperture radar (SAR) experimental results residing in the database are the MSTAR[12] collect, General Atomics Lynx radar data collects at Ku-band with VV polarization and 4-inch resolution, and Sandia test-bed radar data collects at X and Ku-band with varying resolutions and polarizations. These are 4-inch, 1-foot, and 1.5-foot resolution, and HH, HV, and VV polarization. The scene clutter for the targets included grass, asphalt, desert with vegetation, fields, clay, gravel, or sand. All targets and clutter were visually inspected to be distinguishable from each other upon entry into the database. The targets we used within the database consisted primarily of large ground vehicles that would be used by organizations. They include military vehicles such as tanks, launchers, armored vehicles, fuelers, trucks, and transporters. The set also includes organizational civilian vehicles such as bulldozers, flat-bed trucks, school buses, trailers, and large pick-up trucks.

3.2. Civilian Passenger Vehicles

The particular data sets that we analyzed from our database did not include civilian vehicles for personal use. Therefore, we conducted limited experiments to augment the work presented by DLR[1, 5-7] to include different vehicle types, lower grazing angles, and different clutter. Experiment #1 consisted of two SAR spotlight mode circle passes. Images were acquired every 10 degrees in azimuth, with a grazing angle of 20 and 30 degrees for each pass and a resolution of 4 inches at Ku-band with horizontal polarization. The targets were 2 trucks, 2 vans, and 1 sedan shown in Table 1. The truck at location 2 had some objects in the bed of the truck, whereas the truck at location 5 was empty. The vehicles were parked at Sandia's radar calibration site, noted in Figure 1, to obtain absolute RCS. All vehicles were in the same orientation relative to the radar for each pass. The scene clutter was desert with short vegetation, which we measured to be Gaussian-distributed with a logarithmic mean RCS of about -35.2 dBsm and normalized reflectivity of -16.5 dBsm/m^2. The clutter, which can be observed within the vehicle images in Table 1, is adequate for distinguishing our targets.

Table 1. Experiment #1 Passenger Vehicle Type and Location for Spotlight Circle Mode Collects

	Location 1	Location 2	Location 3	Location 4	Location 5
	Chevrolet Express	Ford F350	Pontiac Grand Am	Dodge Caravan	Dodge Ram
	Large Van	Large Truck	Mid-size Sedan	Mid-size Van	Mid-size Truck
Vehicle					

We note that the RCS of motorcycles and sport utility vehicles have yet to be analyzed in the literature or through this work. Such vehicles are recognized as an important target type to include in the larger scope of civilian vehicle RCS characteristics. However, given the limited scope of our experiment, we leave these targets for future work.

4. GROUND VEHICLE RCS MEASUREMENT RESULTS

The ground vehicle RCS experimental data sets described in the prior section are analyzed next.

4.1. Typical SAR Image Chips of Ground Vehicles

In order to understand what the RCS variation of a ground vehicle might look like, we examine a column of derelict M-47 tanks on Kirtland AFB near Albuquerque, New Mexico as shown in the photograph in Figure 2. A series of SAR images of four of those tanks, taken at about 17-degree grazing (ψ) and 30 degrees of variation in squint angle (θ) are shown in Table 2. These are 4-inch resolution, Ku-band, VV-polarization images produced by a prototype Lynx SAR on February 8, 1999. In these images, near range is towards the bottom of the image. Below the SAR image is the sequence of extracted target chips, scaled in RCS units of dBsm with a dynamic range from -20 to 25 dBsm. Note the variation in RCS with angle. In only 2 out of the 28 cases shown, such as the fourth tank at 125-degree squint, does the RCS of a tank demonstrate multiple scatterers of equal strength, indicative of a Swerling 1 target. The majority of the cases, however, show the consistent appearance of a dominant scattering center in red (possibly from a trihedral or dihedral

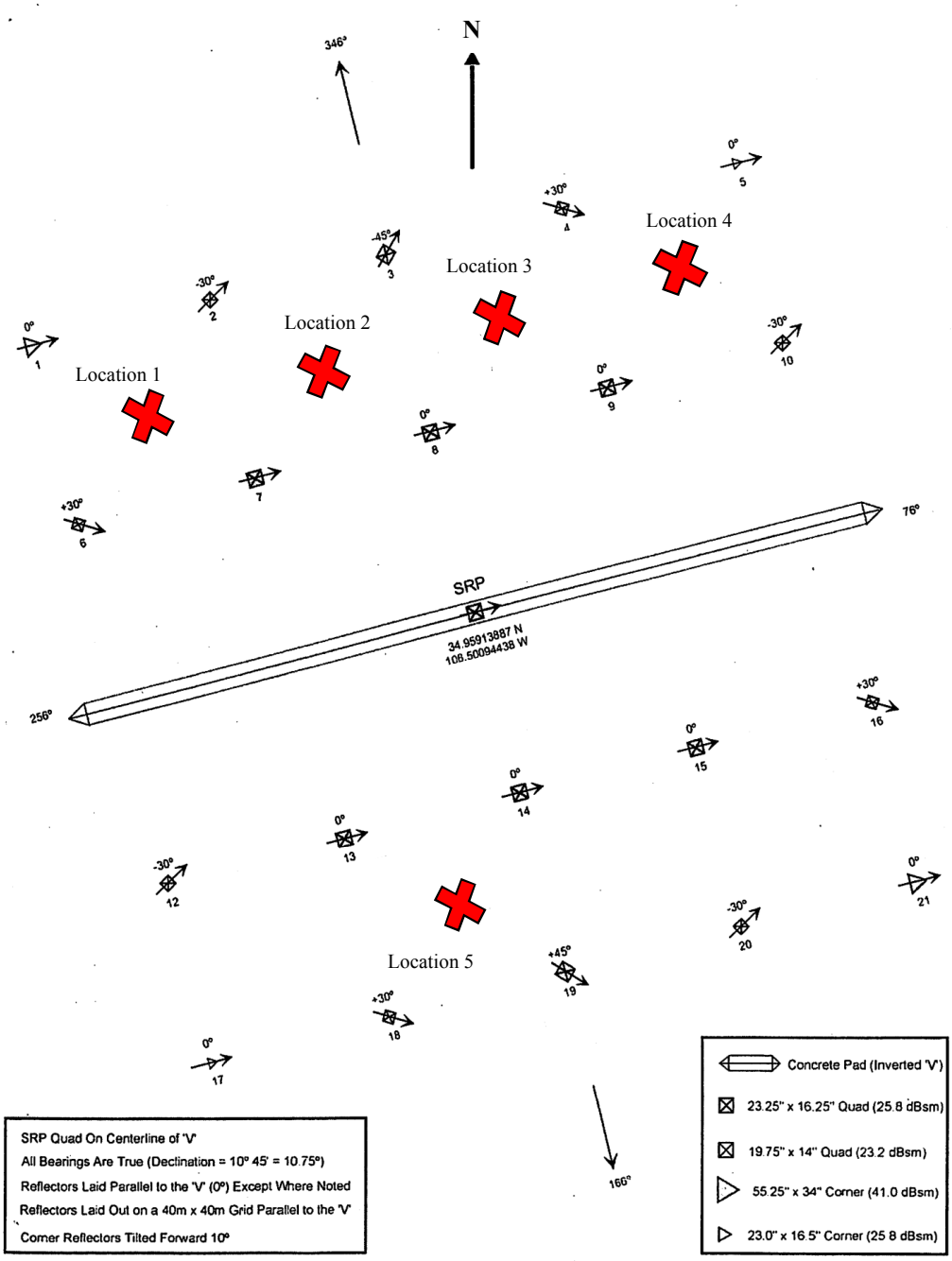

Figure 1. Experiment #1 Passenger Vehicle Target Scene Setup

return from the turret and top base of the tank) amongst the many scatterers, which is indicative of a Swerling 3 target. Civilian ground vehicles demonstrate similar scattering traits, as can be noted by the SAR image chips in Table 3 of our spotlight circle pass experimental data set. The chips selected are of an oblique angle and the cardinal angles of the front, rear, and side of the vehicle. The latter angles prominently show dihedral flashes, particularly for the side and rear of the vehicles. Note the trihedral response from the corner of the truck bed at the oblique angle side view. Also note that the vehicle silhouette is most recognizable, from a human perspective, at oblique angles by observation of the vehicle shadow.

Figure 2. Photograph of Derelict M-47 Tanks

Table 2. Derelict M-47 Tanks SAR Image and Corresponding RCS Returns from Image Chips

Ψ = 17.3 □ Θ = 85.3 □	Ψ = 17.6 □ Θ = 91.5 □	Ψ = 17.2 □ Θ = 100.6 □	Ψ = 16.6 □ Θ = 106.7 □	Ψ = 16.0 □ Θ = 108.5 □	Ψ = 15.3 □ Θ = 113.5 □	Ψ = 14.3 □ Θ = 124.9 □

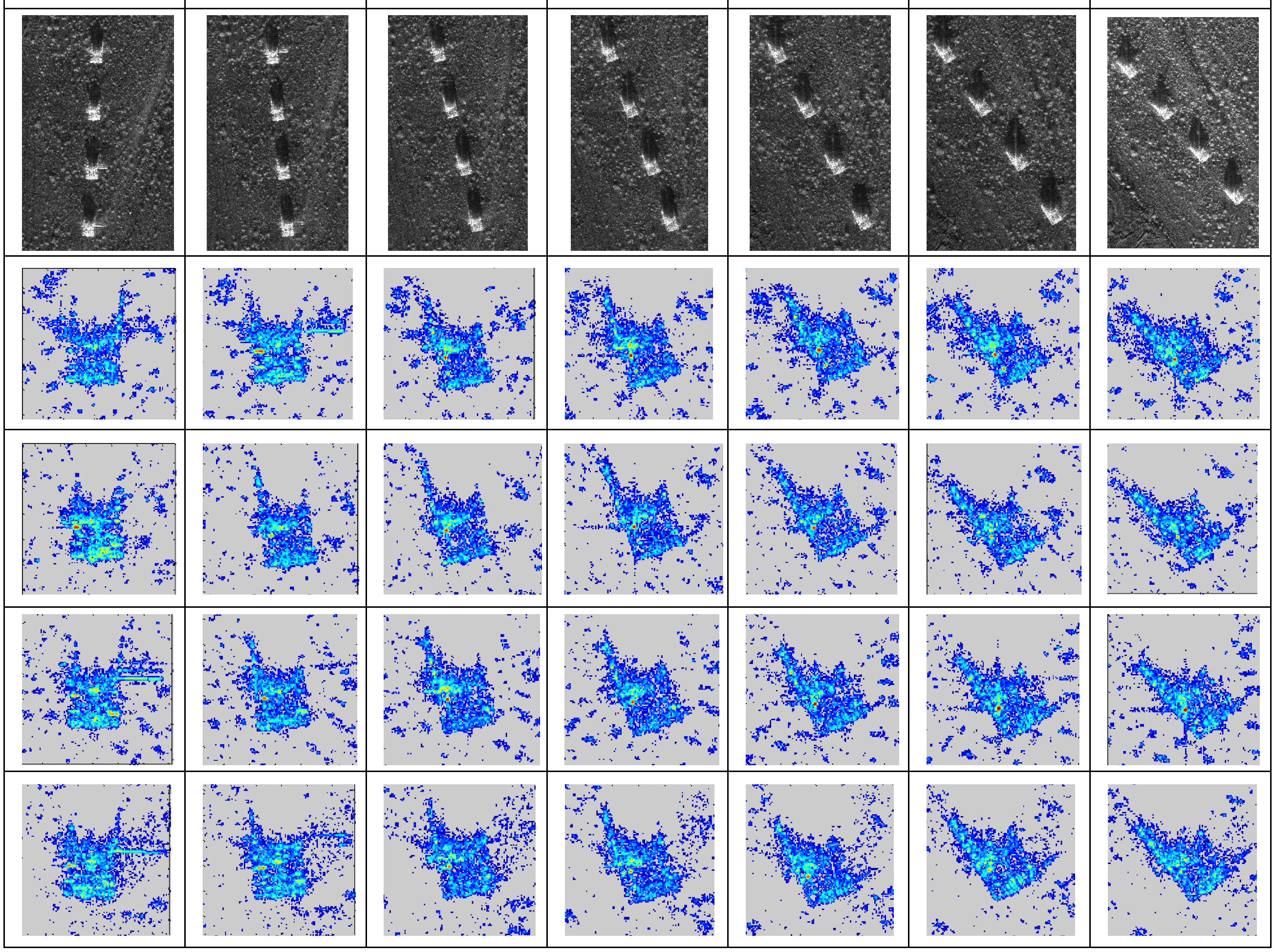

Table 3. SAR Image Chips of Civilian Vehicles at Cardinal and Oblique Angles

	Sedan	Truck	Van
Side Oblique Angle	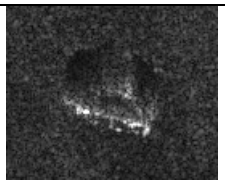	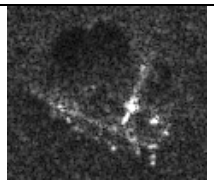	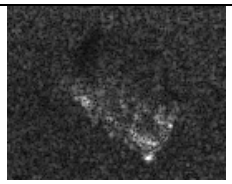
Rear and Front Cardinal Angle	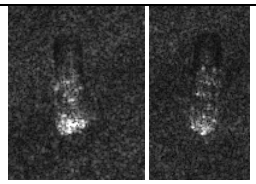	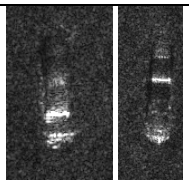	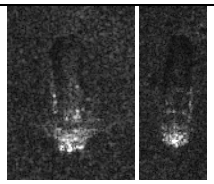
Side Cardinal Angle	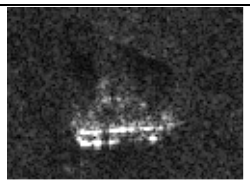		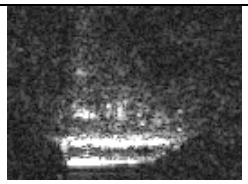

4.2. Ground Vehicle RCS Distribution and Statistics Methodology

We assumed a peak detection algorithm for our ground vehicle RCS measurements. The maximum RCS pixel value in dBsm of each ground vehicle's backscatter return was selected and compiled to generate a probability density function (PDF). The PDF was then integrated numerically to find the cumulative distribution function (CDF) for the data set. We extracted several statistics from our results: 1) the geometric or logarithmic average, 2) the standard deviation of the PDF, 3) the arithmetic or linear average, 4) the median, estimated from the CDF where the probability is 0.5, and 5) the distribution dynamic range, estimated in the following manner. We fitted the Swerling 1 (no dominant scatter, pulse-to-pulse correlation) and Swerling 3 (dominant scatterer, pulse-to-pulse correlation) models[13] with the following equations against our PDFs in order to determine the Swerling type:

$$f_{\text{Swerling\_1}}(\sigma) = \frac{1}{\sigma_{\text{avg}}} e^{-\frac{\sigma}{\sigma_{\text{avg}}}} \quad \text{and} \quad f_{\text{Swerling\_3}}(\sigma) = \frac{4\sigma}{\sigma_{\text{avg}}^2} e^{-\frac{2\sigma}{\sigma_{\text{avg}}}},$$

where σ is the actual or instantaneous RCS, σ_{avg} is the average linear RCS of the target over all fluctuations, and $f_{\text{Swerling\_\#}}$ is the chi-square PDF of 2 or 4 degrees for Swerling 1 or 3 targets, respectively. We then captured the minimum RCS threshold and dynamic range required for probabilities of 0.9 to 0.1. For a Swerling 1 or 3 type target, we compute these by determining when $\sigma \geq \sigma_{avg}\beta$, where $\beta_{1,2} = -9.8$ or 3.6 dBsm and $\beta_{3,4} = -5.8$ or 2.9 dBsm, respectively, using:

$$P_{\text{Swerling\_1,2}}\left\{\frac{\sigma}{\sigma_{\text{avg}}} \geq \beta\right\} = e^{-\beta} \quad \text{and} \quad P_{\text{Swerling\_3,4}}\left\{\frac{\sigma}{\sigma_{\text{avg}}} \geq \beta\right\} = (1+2\beta)e^{-2\beta}.$$

We additionally investigated the probability distributions of our Ku-band ground vehicles at a coarser resolution of 10 meters by windowing our 4-inch resolution data and calibrating the RCS using the brightest corner reflector response in the scene. The return of the vehicle was confined to a smaller number of resolution cells through this process, which is more typical of GMTI radar detection practices.

Statistics	PDF	CDF
Data Set #1 (5º Grazing; HH; 15 Large Vehicles; 1.5' Resolution; X-band; 73,033 Samples with ~90 samples/angle) Log Mean: 7.6 dBsm Arithmetic Mean: 11.9 dBsm Median: 6.2 dBsm Std. Dev.: 4.9 dBsm Range(0.1>P<0.9): 2.1 to 15.5 dBsm Swerling Target: 1 or 3	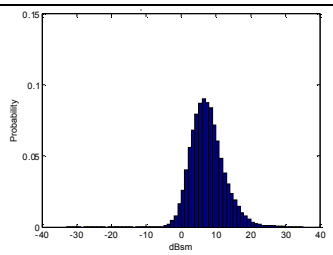	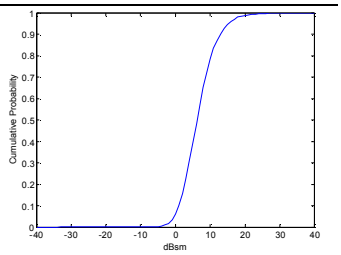
Data Set #2 (5º Grazing; HV; 15 Large Vehicles; 1.5' Resolution; X-band; 73,391 Samples with ~90 samples/angle) Log Mean: -2.3 dBsm Arithmetic Mean: 0.7 dBsm Median: -3.7 dBsm Std. Dev.: 4.1 dBsm Range(0.1>P<0.9): -9.1 to 4.3 dBsm Swerling Target: 1 or 3	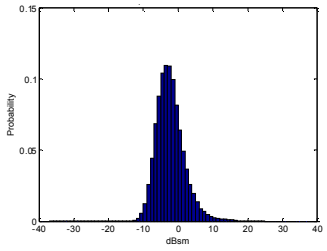	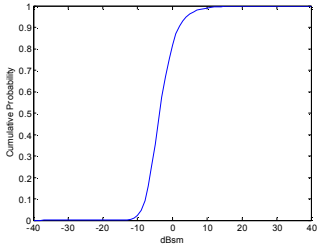
Data Set #3 (5º to 50º Grazing; HH; 37 Large Vehicles; 1' Resolution; X-band; 200,041 Samples with ~36 to 90 samples/angle) Log Mean: 6.5 dBsm Arithmetic Mean: 14.5 dBsm Median: 5.4 dBsm Std. Dev.: 7.9 dBsm Range(0.1>P<0.9): 4.7 to 18.1 dBsm Swerling Target: 1	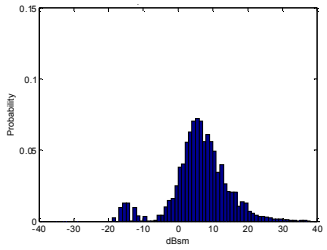	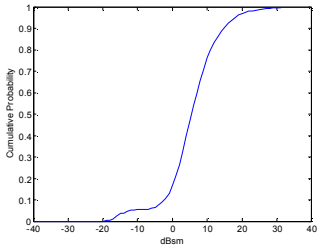
Data Set #4 (10º to 50º Grazing; VV; 18 Large Vehicles; 4" Resolution; Ku-band; 47,697 Samples with ~10 to 40 samples/angle) Log Mean: 15.8 dBsm Arithmetic Mean: 23.9 dBsm Median: 14.1 dBsm Std. Dev.: 8.4 dBsm Range(0.1>P<0.9): 14.1 to 27.5 dBsm Swerling Target: 1	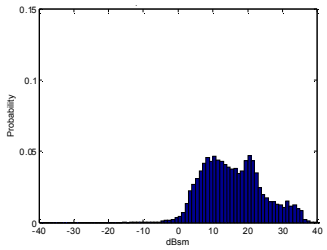	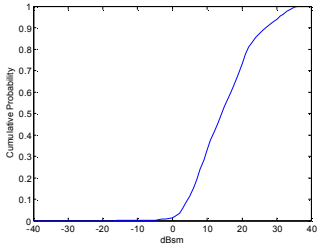
Data Set #5 (20º to 30º Grazing, HH; 5 Civilian Vehicles; 4" Resolution; Ku-band; 360 Samples with ~10 samples / 10º azimuth angle) Log Mean: 2.6 dBsm Arithmetic Mean: 11.4 dBsm Median: 0.7 dBsm Std. Dev.: 8.5 dBsm Range(0.1>P<0.9): 1.6 to 15 dBsm Swerling Target: 1 or 3	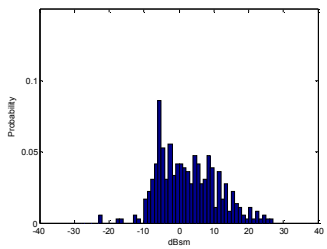	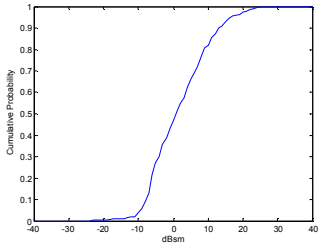
Overall (Data Set #4 & #5 – Ku-band; Many Grazing, Polarization, Clutter, and Vehicle Types; 4" Resolution) Log Mean: 13 dBsm Arithmetic Mean: 22.9 dBsm Median: 11.7 dBsm Std. Dev.: 9.9 dBsm Range(0.1>P<0.9): 13.1 to 26.5 dBsm Swerling Target: 1	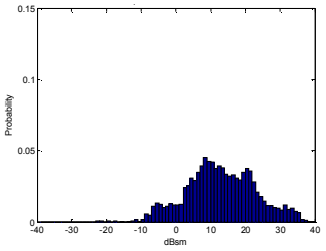	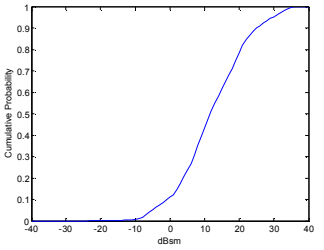

Figure 3. Ground Vehicle RCS Statistics, PDF, and CDF Summary for All Data Sets

4.3. Ground Vehicle Distributions and Statistics for All Data Sets

Figure 3 shows the ground vehicle RCS statistics, PDFs, and CDFs for each data set that we examined. Note that the first three data sets are at X-band. We consider conclusions made at X-band valid at Ku-band based on our observations of the literature[5] that there is minimal frequency dependence in the RCS statistics. The scales on all distributions are the same across results: -40 to 40 for the RCS in dBsm, 0 to 0.15 for the probability, and 0 to 1 for the cumulative probability. In general, the RCS distributions and statistics require qualification and detailed explanations. We will proceed to analyze them in the next sections.

4.4. Effects of Polarization on Ground Vehicle RCS Distributions

Experimental results in the literature[5, 6] indicate that co-polarizations should yield far greater RCS values at similar grazing angles than cross-polarization results. We confirm this observation with our X-band Data Set #1 and #2 where the cross-polarization, HV, median RCS for large vehicles at 5-degree grazing angle is shifted on the order of 10 dB lower than the co-polarization, HH, value. The literature on small civilian vehicle RCS at 42-degree grazing[5, 6] further suggests that cross-polarization RCS is between -15 and 0 dBsm. Our large vehicle RCS distribution at low grazing exhibits RCS values greater than 0 dBsm at HV, though naturally with lesser likelihood. The range of RCS values for our case seems to be bounded by +/- 12 dBsm instead. Additionally, VV and HH co-polarizations should be similar in behavior according to the literature.[3-6] We do not have an adequate data set comparison to confirm these claims based on RCS statistics and merely refer the reader to the results offered by others.

4.5. Effects of Aspect on Ground Vehicle Distributions

Figure 4 shows the variation in the mean RCS value in dBsm as a function of aspect angle for X-band Data Set #1 through #3 of large vehicles. Zero degrees corresponds to the front of the vehicles. The mean RCS is near 7 dBsm and fairly constant as a function of aspect angle (i.e. no more than a 2-3 dB fluctuation) for all oblique angles with HH polarization. The RCS dihedral flashes at the cardinal angles for the front, rear and sides of the vehicles breaks this consistency. The frontal flash appears to be 5 dB lower than the sides, the rear is slightly higher, and the side flash is always the greatest, as we would expect. Overall, the oblique angle mean RCS is roughly 16 dB lower in value than the cardinal angles which range from 10 to 20 dBsm. The cross-polarization angular behavior is substantially different in that the RCS "beamwidth" for the cardinal angle flashes is broadened across angle and the constancy in RCS values at oblique angles is not apparent. The maximum RCS value at the cardinal angles is roughly 18 dB lower at HV than that of HH at the lower grazing angle, reaffirming our prior conclusions between cross and co-polarization RCS. Lastly, we note that our RCS polar plots are in line, both in shape and magnitude, with results presented for a battle tank model and measurements by Papadopoulos[10] and Lees, et al.[9], respectively. Some specifics of their single-target results understandably vary over our generalist, multi-vehicle approach intended for cursory radar system design.

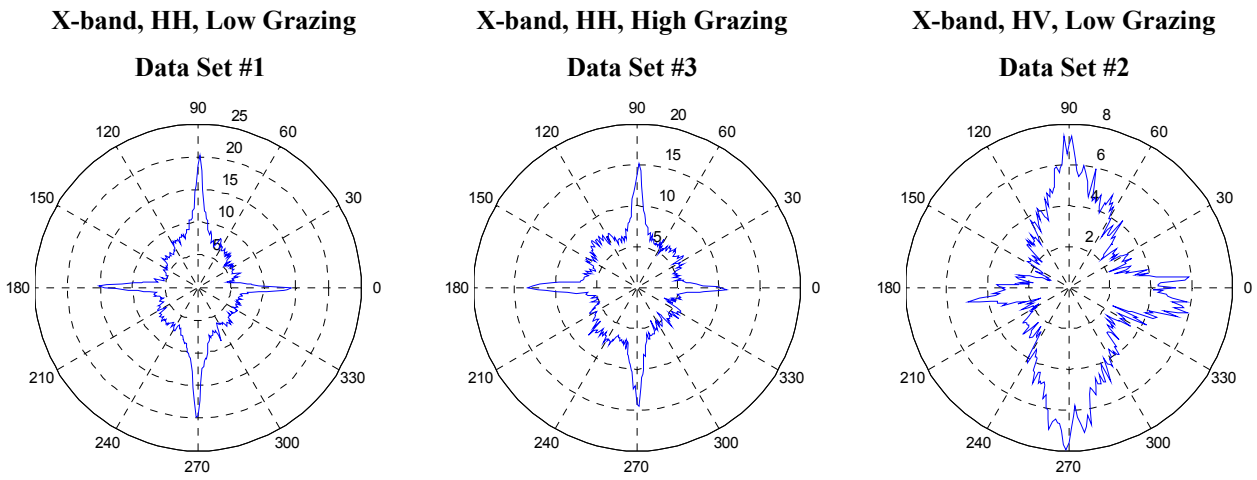

Figure 4. RCS Variation with Aspect Angle (dBsm)

4.6. Effects of Grazing Angle on Ground Vehicle Distributions

If we compare X-band Data Set #1's distributions to those of Data Set #3 in Figure 3, we observe a spreading of the distribution at higher grazing angles given by a 3 dB increase in the standard deviation. Except for the arithmetic mean RCS, the geometric mean and median decrease minimally with increasing grazing angle. These slight differences may partially be due to the fact that the resolution, samples, and targets for Data Set #3 are different. In general, however, the mean RCS seems to vary minimally (within 1 to 2 dB) at oblique angles with changes in grazing angle as can be seen in the elevation and azimuth mean RCS maps of Figure 5. At the cardinal angle flashes, a decrease in the mean RCS occurs by about 5 dB between 5 degrees and 45 degrees of grazing angle. This decrease at the cardinal angles is also apparent in the azimuthal polar RCS plots of

Figure 4. Relative to the standard deviation, however, these minor differences are not statistically significant.

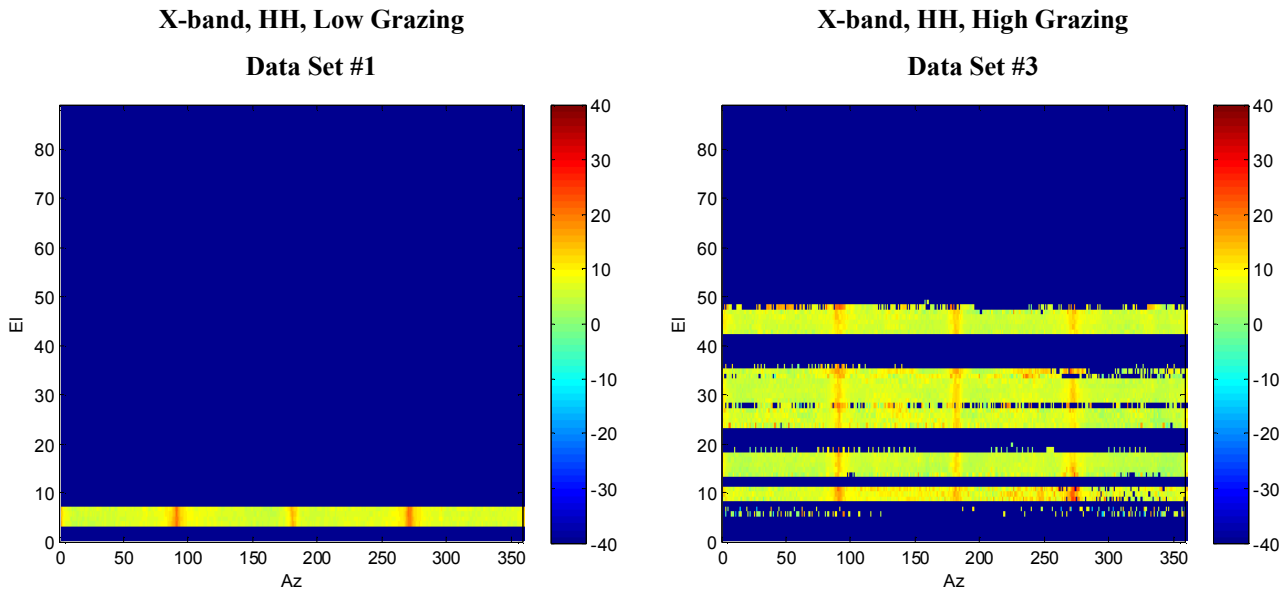

Figure 5. RCS Variation with Grazing Angle (dBsm)

4.7. Effects of Vehicle Type and Size on RCS Distributions

In order to understand the influence of vehicle type and size on the overall RCS distribution, we examine the Ku-band, 4-inch resolution Data Sets #4 and #5 in Figure 3, which represent large organizational vehicles and smaller civilian vehicles, respectively. The small civilian vehicle distribution is shifted roughly 13 dB lower than the large vehicle distribution, given that their medians are 0.7 dBsm and 14.1 dBsm, respectively. However, both distributions are similar in their relative range of 40 dB with a standard deviation of about 8.5 dB and their PDF shape, which is non-Gaussian. The downward shift in the median RCS is a clear indicator that the distribution of a set of vehicles is largely dependent on the sizes of the vehicles comprising it.

The non-Gaussian shape of the distribution requires further study. We refer to Figure 6 and Figure 7, which show the PDF and RCS statistical values for the civilian vehicle experiment, broken down by each vehicle. Care should be taken when making detailed conclusions about these distributions, as the number of samples is rather low at 72 samples. Nonetheless, we generally observe that the sedan and the vans have distributions in the range of -10 to 10 dBsm, whereas the trucks are shifted toward a positive range. This behavior is likely due to predominant trihedral and dihedral scattering from the truck bed. These scattering mechanisms are unavailable for the smoother and less retro-reflective vans and sedans. Additionally, we observe that the size of the vehicle is particularly important to the distribution, since the sedan has a PDF that is skewed towards -10 dBsm; the vans are centered near 0 dBsm; and the maximum range of the large

truck reaches 26 dBsm, whereas the small truck's distribution ends near 16 dBsm. The combination of such diverse RCS statistics into one overall distribution explains the large spread in range and non-Gaussian shape of the distributions for Data Sets #4 and #5. Furthermore, data set sampling bias may influence the distribution's shape. We removed any single target sampling bias from the distributions (e.g. more T-72 samples than M-47 samples). However, we did not attempt to compensate for sampling bias per target type (e.g. more tank targets than transporters causing a bias toward tank targets), which admittedly can also impact the distribution shape. We also did not compensate for angular sampling bias, but our data sets did not seem to merit this need, despite a non-uniform number of samples per angle. The variation was within 15 samples, and generally the larger sampling bias occurred at oblique angles, where the RCS is fairly constant.

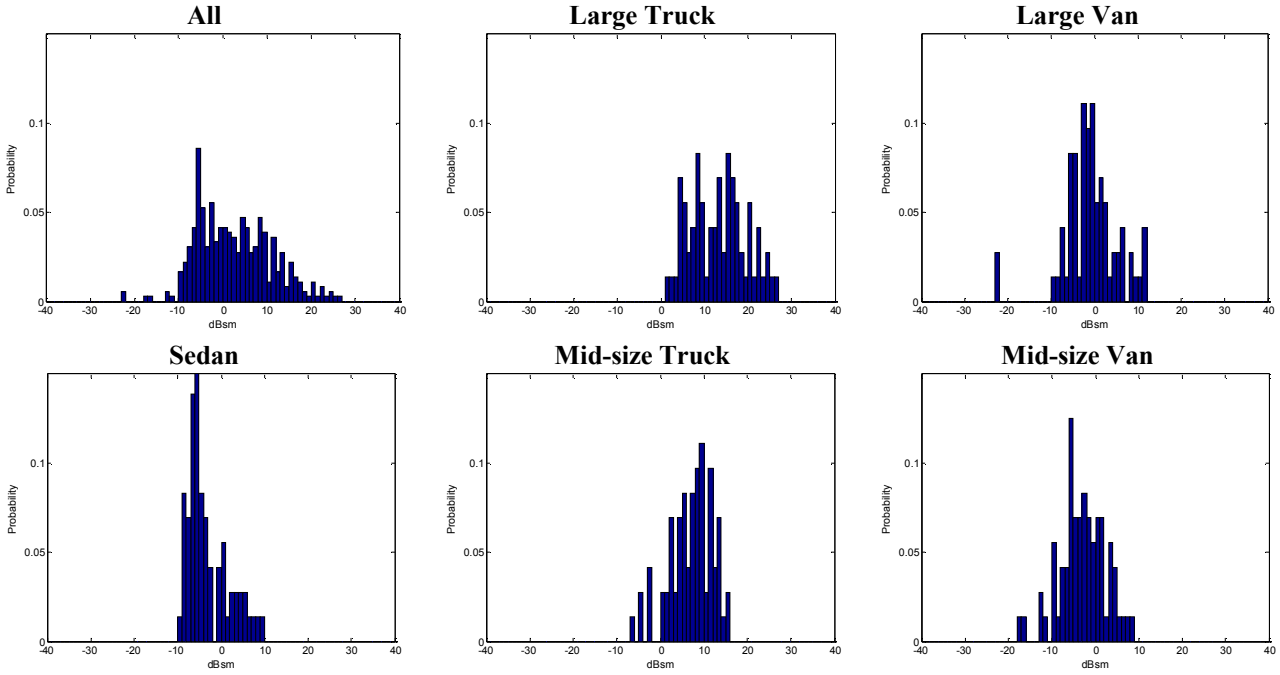

Figure 6. Civilian Ground Vehicle Experiment RCS PDF versus Vehicle Type

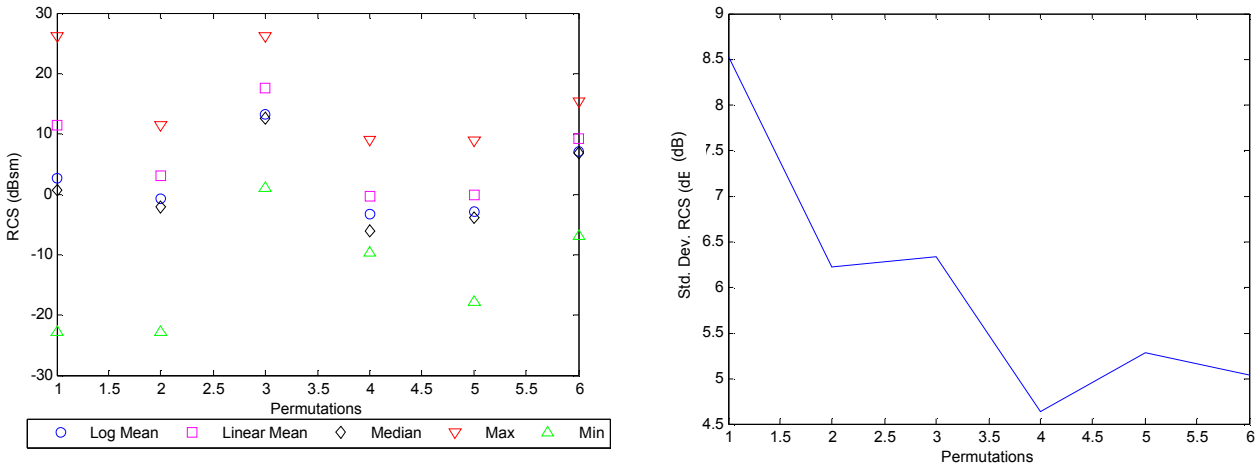

Vehicle Type Permutations: 1. All, 2. Large Van, 3. Large Truck, 4. Sedan, 5. Mid-size Van, 6. Mid-size Truck

Figure 7. Civilian Ground Vehicle Experiment RCS Statistical Values Across Vehicle Type

4.8. Effects of Resolution on Ground Vehicle RCS Distributions

The PDF and CDF at 10-meter resolution, as well as their statistics, are approximately 10 dB stronger than the 4-inch resolution data for our Ku-band results according to Figure 8. These results are expected when we consider that the backscatter energy of the target is concentrated in one to a few resolutions cells for the coarser resolution case. For ground vehicles, a stronger value for the RCS at all aspect angles seems to result for the complex average of many scattering centers (and clutter) within a single resolution cell versus the average of a few scattering centers (and clutter) within a resolution cell. This result is not true in general for all targets. However, ground vehicles naturally have a distributed scattering return among many resolution cells by virtue of the vehicles' sheer physical size relative to the radar wavelength (as can be seen in Table 2 and Table 3). When the resolution cell size is expanded to encompass the entire target return within a single cell (and additional clutter), a larger RCS value generally results. The overall shape and spread of the coarse resolution distributions changes somewhat as compared to the 4-inch resolution data sets. This behavior is not unreasonable given that the RCS is being computed over a resolution cell that is two orders of magnitude larger than before. How the target's scatterers interact complexly at such diverse scales along with clutter to yield the RCS of the target is non-linear, nevermind the fact that we are combining several targets in one distribution and may have target type sampling bias. The overall ranges and standard deviations of our distributions are comparable to the general comments in the literature, particularly for large vehicles.

Statistics	PDF	CDF
Data Set #6 (10° to 50° Grazing; VV; 18 Large Vehicles; Ku-band; 46,820 Samples with ~10 to 40 samples/angle; 10m Resolution) Log Mean: 20.1 dBsm Arithmetic Mean: 28.5 dBsm Median: 22.9 dBsm Std. Dev.: 11.8 dBsm Range(0.1>P<0.9): 18.7 to 32.1 dBsm Swerling Target: 1	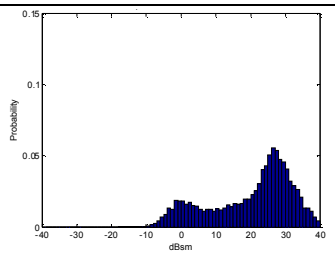	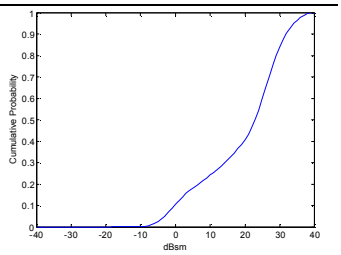
Data Set #7 (20° to 30° Grazing, HH; 5 Civilian Vehicles; Ku-band; 360 Samples with ~10 samples / 10° azimuth angle; 10m Resolution) Log Mean: 13.5 dBsm Arithmetic Mean: 17.7 dBsm Median: 11.9 dBsm Std. Dev.: 5.6 dBsm Range(0.1>P<0.9): 7.9 to 21.3 dBsm Swerling Target: 1 or 3	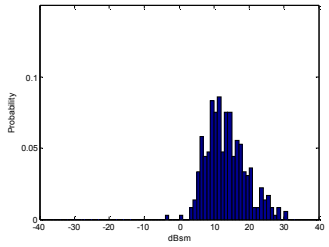	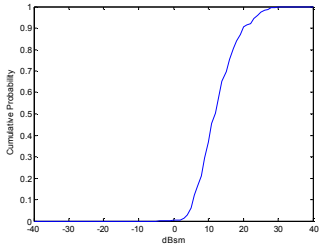
Overall (Data Set #6 & #7 – Ku-band; Many Grazing, Polarization, Clutter, and Vehicle Types; 10m Resolution) Log Mean: 18.7 dBsm Arithmetic Mean: 27.5 dBsm Median: 19.4 dBsm Std. Dev.: 11.1 dBsm Range(0.1>P<0.9): 17.7 to 31.1 dBsm Swerling Target: 1	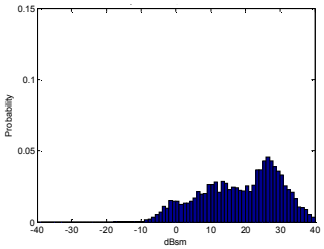	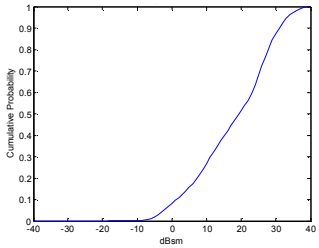

Figure 8. Ground Vehicle RCS Statistics, PDF, and CDF Summary for Coarsened Resolution of 10m

4.9. Ground Vehicle RCS Swerling Target Models

How a target's RCS fluctuates as a function of angle is important for setting algorithm probability of detection and false alarm thresholds.

Figure 9 shows the Swerling target 1 and 2 models normalized against the overall ground vehicle PDF for both 4-inch and 10-meter resolutions. The x-axis is in logarithmic scale due to the fact that the distribution tails for ground vehicles are quite long because of the strong flashes at cardinal angles. The number of bins for the distribution was established by the square-root of the number of samples. The Swerling 1 target model best fits the overall PDF of both resolutions.

The target signature of a ground vehicle is comprised of multiple scatterers with one usually being dominant, as seen in the SAR image chips, which would indicate a Swerling 3 target. However, in some instances across aspect angle, the signature is comprised of multiple scatterers of similar strength, which would indicate a Swerling 1 target. One could argue that the cardinal angle flashes constitute this latter case more so than the former for ground vehicles. The resolution cell size further impacts whether these scatterers are distinguishable across aspect or whether the scatterers are conglomerated and averaged into one cell (which leans toward a Swerling 1 target). Consequently, the Swerling 1 model results are as expected at coarse resolutions such as 10 meters.

The fact that a Swerling 1 model also best fits the 4-inch resolution data set is surprising and requires further investigation. The Swerling 1 model is only marginally a better fit than Swerling 3 in this case. This observation is more clearly noted in Figure 10, which shows the Swerling model fit for Data Set #1. The Swerling fit is ambiguous in this case when we take the full range of RCS samples. However, by eliminating the RCS samples that exceed 90% probability in the CDF, which yield the long tails and primarily constitute the cardinal angle results of the vehicle RCS, then the Swerling 3 model fits best. This result makes intuitive sense, since Swerling 3 characteristics are predominantly observed in the oblique angles of the SAR image chips. Furthermore, this observation holds with all of our data sets. In sum, there is a necessary tradeoff in system design for the detection of ground vehicles. The Swerling 3 model is more restrictive on detection thresholds than Swerling 1. The likelihood of the target truly being a Swerling 1 is limited to a small number of angles. If Swerling 3 is chosen, the probability of false alarm is less, but that of a missed detection is greater. Yet, Swerling 3 is more forgiving toward the dynamic range requirements of a radar design (i.e. signal-to-noise ratio). If Swerling 1 is chosen, then the converse is true. Given that the pose of the target is generally unknown, the conservative approach of selecting Swerling 1 for all cases and designing a radar with greater dynamic range is more favorable from a detection standpoint. These observations are affirmed by Skolnik[14] for most man-made targets, not just ground vehicles.

We also note that the ground vehicle distributions are chi-square, since that is the implicit assumption for the Swerling target 1 and 3 PDFs, which we have fitted to our data set. Furthermore, the degree of freedom for the chi-square distribution is 2 for the overall ground vehicle distributions, since that many degrees of freedom are required for the Swerling 1 model. If a Swerling 3 model were chosen, the degrees of freedom would be 4.

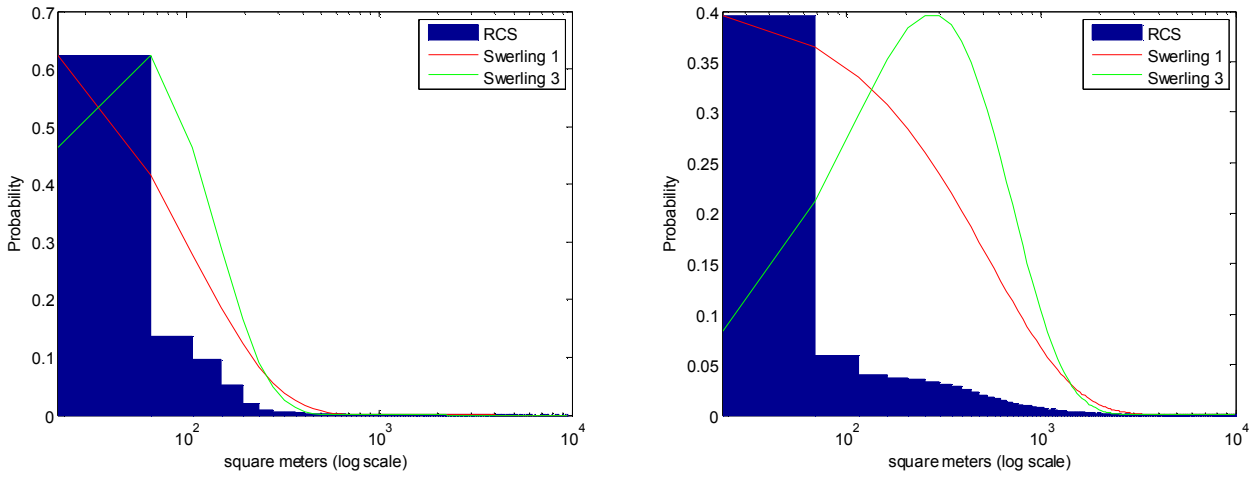

Figure 9. Swerling Models Fitted to PDFs of Ground Vehicles for Overall Data Sets at Ku-band

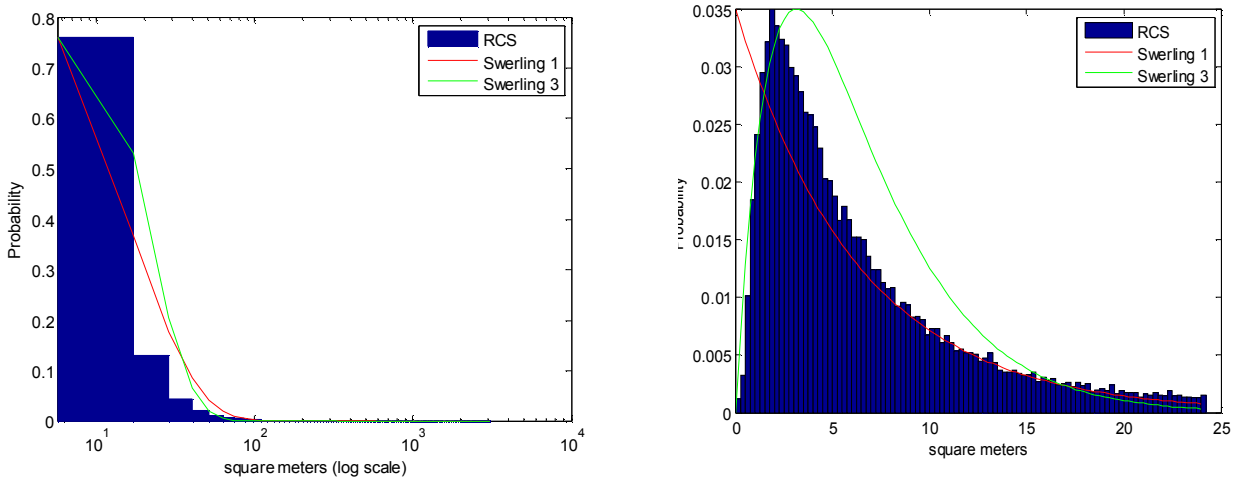

All RCS Samples **RCS Samples Below 90% in CDF**

Figure 10. Swerling Models Fitted to PDF of Ground Vehicles for Data Set #1 Over Specific Samples

4.10. Overall Ground Vehicle RCS Distributions

We refer to the overall statistics of ground vehicles at 4-inch and 10-meter resolution for all vehicle types, sizes, configurations, poses, polarization, and clutter of our data sets at the bottom of Figure 3 and Figure 8. The geometric average RCS is 13 and 18.7 dBsm, with standard deviations of 9.9 and 11.1 dB for 4-inch and 10-meter resolution, respectively. The ground vehicles exhibit a Swerling 1 target model. The overall RCS probability distribution range of values varied from about -10 to 40 dBsm for both resolutions. We conclude that a minimum detection threshold of 13.1 dBsm at 4-inch resolution and 17.7 dBsm at 10-meter resolution is required to achieve the likelihood of detecting a ground vehicle 90% of the time. Similarly, we capture the dynamic range, noting that there is a 10% chance the ground vehicle RCS will be above 26.5 dBsm and 31.1 dBsm for 4-inch and 10-meter resolution, respectively. The probability distributions of the ground vehicles validate these expectations. The existing literature on both military and civilian vehicles confirms these results in general, particularly for large vehicles, which compose the majority of our data set samples.

5. CONCLUSIONS

We examined the RCS probability distributions of different ground vehicle sizes, types, and configurations, across aspect and elevation angle, polarization, resolution, and clutter from experimental data sets at X and Ku-band. We leveraged results in the existing literature that VV polarization is approximately similar to HH, and there is minimal frequency dependence across radiolocation bands.

At X-band and with a large vehicle data set at 1.5-foot resolution, we demonstrated that the RCS of ground vehicles is 10 dB lower for HV than HH polarization. The RCS varied with aspect angle in a predictable pattern. Oblique angles of the target exhibited a reasonably constant mean RCS near 7 dBsm, but cardinal angles from front, rear, and side scattering of the vehicles peak (in increasing order) at 10 to 20 dBsm. The pattern for cross-polarizations exhibited broadened cardinal angle peaks without the constant RCS at oblique angles. The RCS was reasonably consistent as a function of grazing angle, with a 5 dB decrease with increasing angle from 5 to 45 degrees.

At Ku-band with 4-inch resolution, we noted that a large vehicle size shifts the RCS distribution up by 13 dB for our organizational, large targets versus smaller, civilian vehicles. Within the civilian vehicle distribution we further noted that trucks have a wide range of RCS values from -10 to 30 dBsm due to strong dihedral and trihedral scattering from the

truck bed at most angles, whereas most other vehicles such as vans and sedans have ranges from -10 to 10 dBsm. Combining such diverse targets into one probability distribution yields a non-Gaussian shape for the PDF.

Likewise at Ku-band, we observed the RCS behavior as a function of resolution cell size and determined a Swerling model fit for our distributions. According to the SAR image chips of select vehicles, a Swerling 3 target with multiple scattering centers and one being dominant tended to be the norm at most angles. Occasionally, and particularly at cardinal angles where strong flashes occurred, vehicles exhibited a Swerling 1 behavior that lead to very long tails in the RCS distribution. A large resolution cell size, such as 10 meters, where the entire target was within a single cell produced a 10 dB increase in the RCS than the 4-inch case. Swerling 1 target behavior of ground vehicles tended to be observed as the most general case for all data set distributions and parameter variations, though it only applies at limited angles. Swerling 3 target behavior can be applied to a significant percentage (on the order of 90%) of the RCS samples (and poses) of a ground vehicle due to the aforementioned scattering behavior for all data sets. The choice of Swerling model is left to the radar designer based on signal-to-noise ratio, probability of detection, and probability of false alarm performance requirements, though the recommended conservative approach is to use a Swerling 1 target model.

Geometric mean, standard deviation, median, arithmetic mean, and range varied depending on all of these vehicle, radar, and collection scenario parameters. However, overall for HH or VV polarization with both large and small vehicles, the distribution characteristics (in the order mentioned) were: 13 dBsm, 9.9 dB, 11.7 dBsm, 22.9 dBsm, and -10 to 40 dBsm for 4-inch resolution. At 10-meter resolution, the much stronger RCS results were: 18.7 dBsm, 11.1 dB, 19.4 dBsm, 27.5 dBsm, and -10 to 40 dBsm, respectively. The target RCS fluctuations across look angle were found to be characteristic of a Swerling 1 target for both resolutions. Detection thresholds for a 90% probability of detection were determined to be 13.1 dBsm and 17.7 dBsm for 4-inch and 10-meter resolution, respectively. RCS values for which the ground vehicle RCS had a 10% probability of exceeding that value were determined to be 26.5 and 31.1 dBsm for 4-inch and 10-meter resolution, respectively. Thus, expectations for radar algorithm design and performance for ground vehicle detection can be appropriately established. Good agreement was noted between simulation and experimental observations in the existing literature and our experimental data sets for polarization, aspect angle, and general RCS statistical behavior of ground vehicles.

ACKNOWLEDGMENTS

This report was funded by General Atomics Aeronautical Systems, Inc. (ASI) Reconnaissance Systems Group (RSG). The authors would also like to thank the Sandia National Laboratories (SNL) for kindly allowing us to use the synthetic aperture radar automatic target recognition database. Finally, this study would not have been possible without the coordination and participation of Michael N. Taylor and many other members of the Sandia ground team for an additional collect in 2011 with their Ku-band test-bed radar system.

Sandia National Laboratories is a multi-program laboratory managed and operated by Sandia Corporation, a wholly owned subsidiary of Lockheed Martin Corporation, for the U.S. Department of Energy's National Nuclear Security Administration under contract DE-AC04-94AL85000.

GA-ASI, an affiliate of privately held General Atomics, is a leading manufacturer of Unmanned Aircraft Systems (UAS), tactical reconnaissance radars, and surveillance systems, including the Predator® UAS-series and Lynx radar.

REFERENCES

[1] G. Palubinskas and H. Runge, "Radar signatures of a passenger car," *IEEE Geoscience and Remote Sensing Letters*, vol. 4, no. 4, Oct. 2007.

[2] W. E. Nixon, H. J. Neilson, G. N. Szatkowski, R. H. Giles, W. T. Kersey, L. C. Perkins, and J. Waldman, "A variability study of Ka-band HRR polarimetric signatures on eleven T-72 tanks," *Proceedings of the SPIE Conference on Algorithms for Synthetic Aperture Radar Imagery V*, vol. 3370, pp. 369-382, Orlando, FL, 14 Apr. 1998

[3] R.H. Giles, W.T. Kersey, M.S. McFar1in, R. Fin1ey, H.J. Neilson, and W.E. Nixon, "A study of target variability and exact signature reproduction requirements for Ka-Band radar data," *Proceedings of the SPIE Conference on Signal Processing, Sensor Fusion, and Target Recognition X*, vol. 4380, pp. 117-126, Orlando, FL, 16 Apr. 2001.

[4] T. M. Goyette, J. C. Dickinson, C. Beaudoin, A. J. Gatesman, R. Giles, J. Waldman, and W. E. Nixon, "Acquisition of UHF and X-Band ISAR imagery using 1/35th scale-models," *Proceedings of the SPIE Conference on Algorithms for Synthetic Aperture Radar Imagery XII*, vol. 5808, pp. 440-449, Orlando, FL, 28 Mar. 2005.
[5] G. Palubinskas, H. Runge, and P. Reinartz, "Radar signatures of road vehicles," *Proceedings of the 2004 IEEE International Geoscience and Remote Sensing Symposium, IGARSS '04*, vol. 2, pp. 1498-1501, Anchorage, Alaska, Sept. 20-24, 2004.
[6] G. Palubinskas, H. Runge, and P. Reinartz, "Measurment of radar signatures of passenger cars: airborne SAR multi-frequency and polarimetric experiment," *IET Radar, Sonar, and Navigation*, vol. 1, no. 2, pp. 164-169, 2007.
[7] G. Palubinskas, H. Runge, and P. Reinartz, "Radar signatures of road vehicles: airborne SAR experiments," *Proceedings of SPIE*, vol. 5980, 2005.
[8] M. Haruta, H. Ishizaka, O. Hashimoto, J. Ueyama, and K. Wada, "Measurement of radar cross section for a truck and bus under an open field in 60 GHz band," *Microwave and Optical Technology Letters*, vol. 25, no. 4, pp. 243-246, May 20, 2000.
[9] P. A. Lees and M. R. Davies, "Computer prediction of RCS for military targets," *IEE Proceedings*, vol. 137, part F, no. 4, pp. 229-236, Aug. 1990.
[10] S. Papadopoulos, A. K. Mishra, and B. Mulgrew, "Monostatic radar signatures of significant classes of ground targets, in the time and frequency-domain," *Proceedings of the 3rd European Radar Conference*, pp. 96-99, Sept. 2006.
[11] S. Papadopoulos and B. Mulgrew, "Scenario based RCS statistics of complex ground targets," *IEEE*, 2008.
[12] MSTAR Data Set: https://www.sdms.afrl.af.mil/index.php?collection=mstar.
[13] P. Swerling, "Probability of detection for fluctuating targets", *IRE Transactions on Information Theory*, vol. 6, issue 2, pp. 269-308, 1960.
[14] M. L. Skolnik, *Introduction to Radar Systems, 3rd Ed.*, McGraw Hill, New York, 2001.